

Electronic Supplementary Information

Sulfur Doped FeO_x Nanosheet Arrays Supported on Nickel Foam for Efficient Alkaline Seawater Splitting

Weiju Hao^a, jinli Fan^a, Xia Xu^{a*}, Yiran Zhang^a, Haiyang Lv^a, Shige Wang^a, Shengwei Deng^c, Shuo Weng^{a*}, Yanhui Guo^{b*}

^aUniversity of Shanghai for Science and Technology, Shanghai, 200093, China.

^bFudan University, Shanghai 200433, P. R. China

^cCollege of Chemical Engineering, Zhejiang University of Technology, Hangzhou, 310014, China

* Corresponding authors.

E-mail: ecustwengs@163.com

gyh@fudan.edu.cn

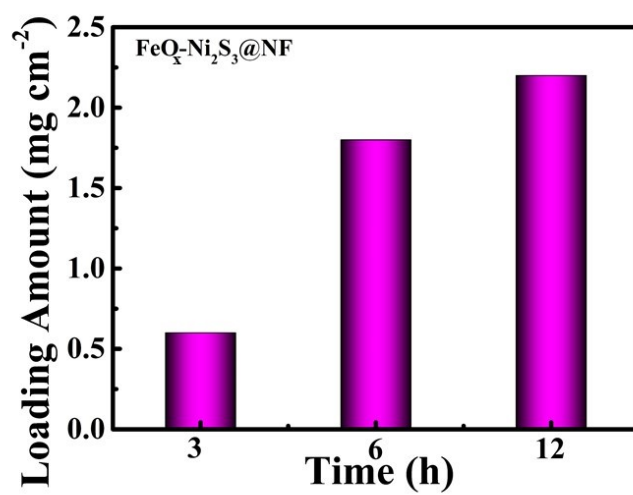


Figure S1. The loading amount of FeO_x-Ni₃S₂ catalyst material on NF at 3 h, 6 h and 12 h, respectively.

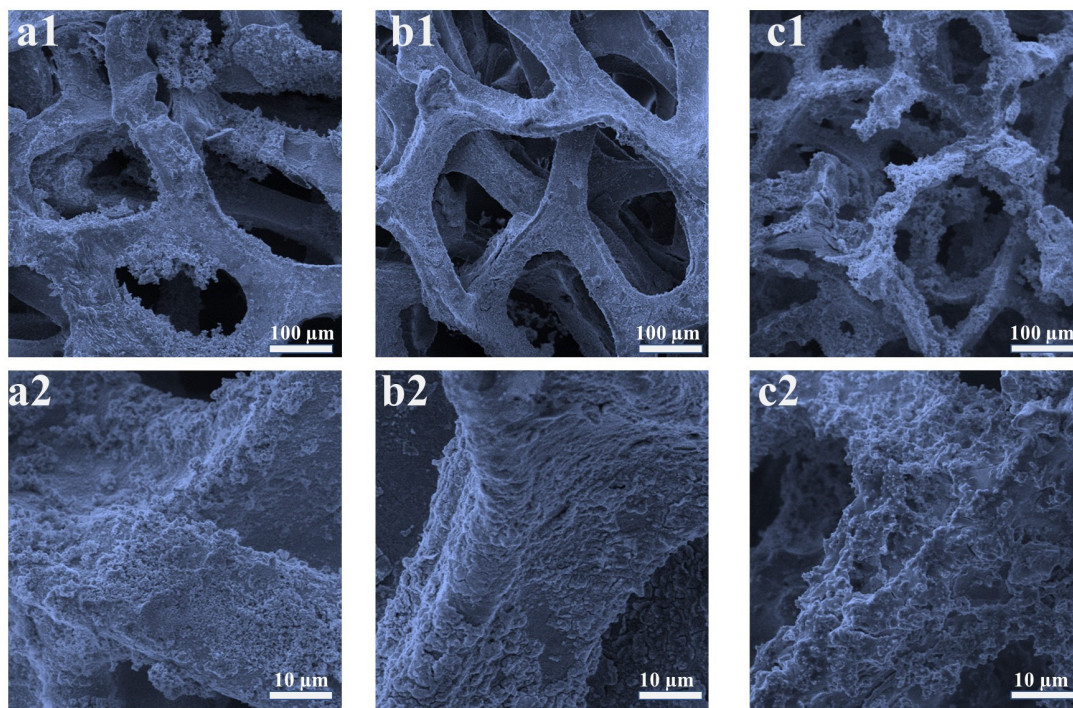


Figure S2. FESEM images of the $\text{FeO}_x\text{-Ni}_3\text{S}_2\text{@NF}$ composite with hydrothermal for (a) 3 h, (b) 6 h and (c) 12 h.

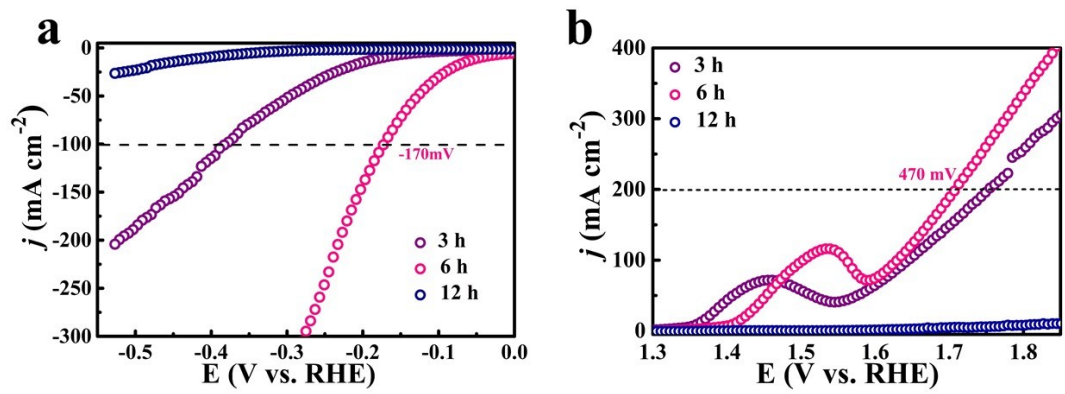


Figure S3. LSV curves of FeO_x-Ni₃S₂@NF for HER (a) and OER (b) in 1.0 M KOH+0.5 M KOH with different hydrothermal time.

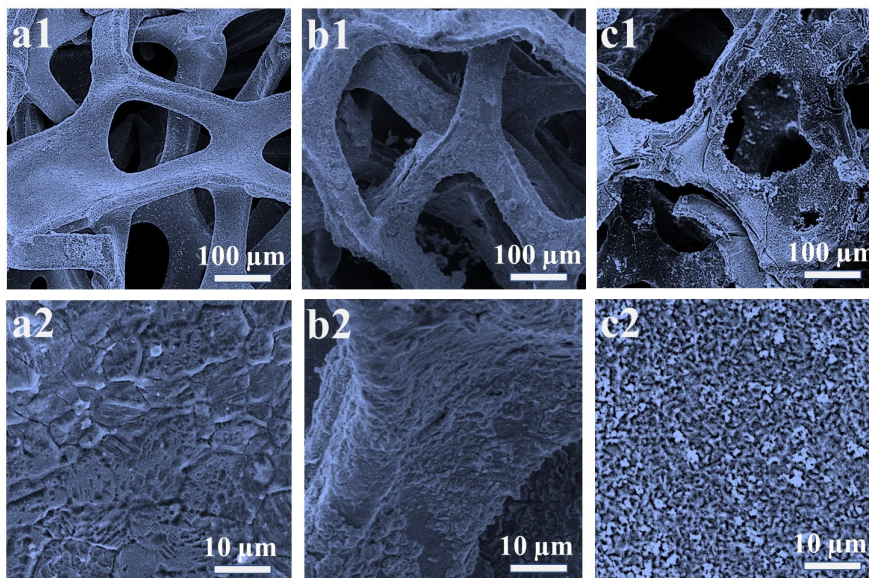


Figure S4. The influence of the amount of thiourea doping on the morphology. (a) Without S; (b) Fe:S=1:1; (c) Fe:S=1:2.

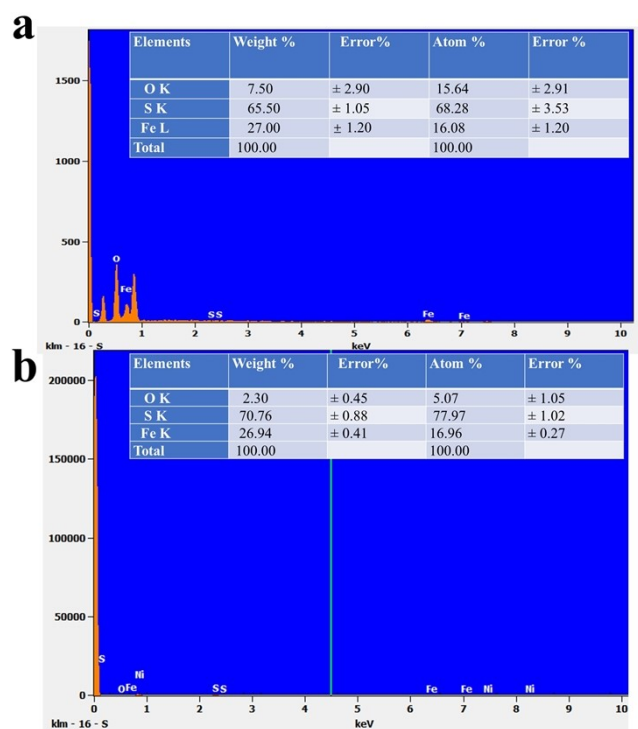


Figure S5. The influence of the amount of thiourea doping on the composition of $\text{FeO}_x\text{-Ni}_3\text{S}_2@\text{NF}$. (a) Fe:S=1:1; (b) Fe:S=1:2.

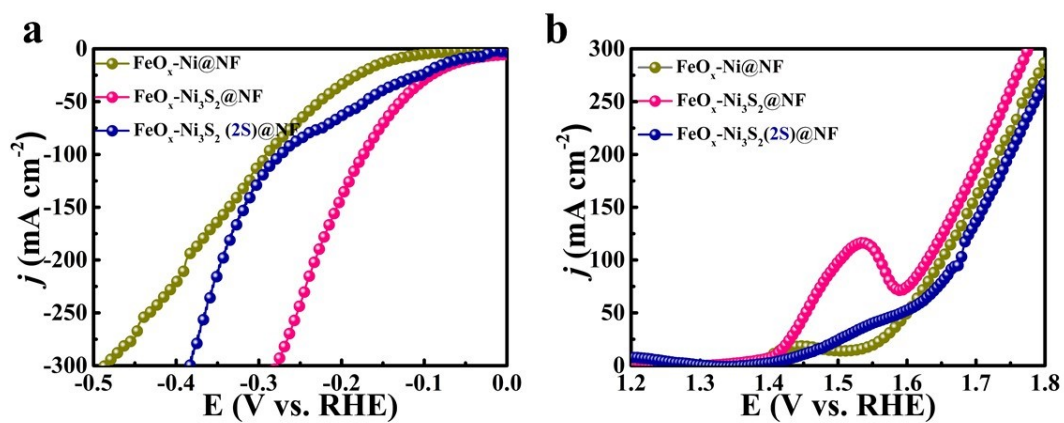


Figure S6. Polarization curves of FeO_x-Ni@NF for HER (a) and OER (b) in 1.0 M KOH with different sulfur source doping amount.

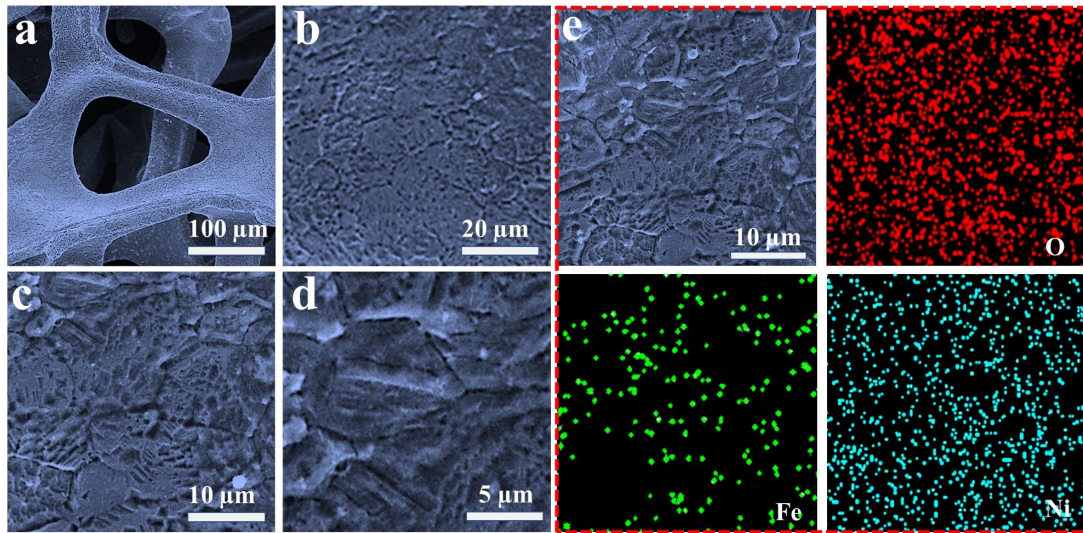


Figure S7. FESEM (a-d) and EDS (e) mapping images of $\text{FeO}_x\text{-Ni@NF}$ electrode.

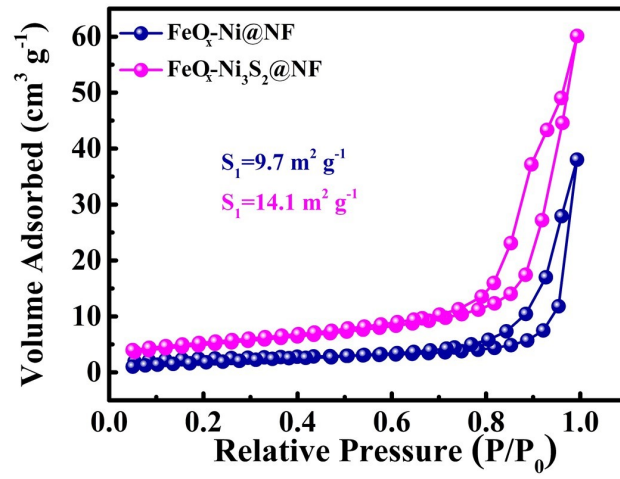


Figure S8. Nitrogen isotherms of the FeO_x-Ni@NF and FeO_x-Ni₃S₂@NF electrodes in nitrogen.

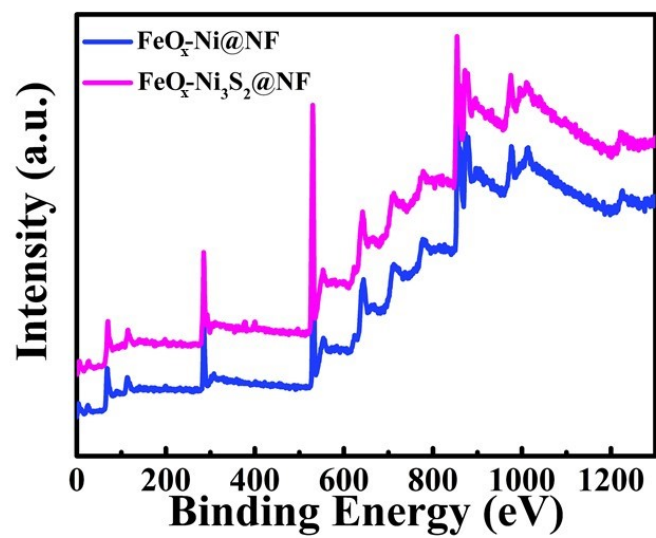


Figure S9. The survey XPS spectrum of the $\text{FeO}_x\text{-Ni@NF}$ and $\text{FeO}_x\text{-Ni}_3\text{S}_2\text{@NF}$ composite.

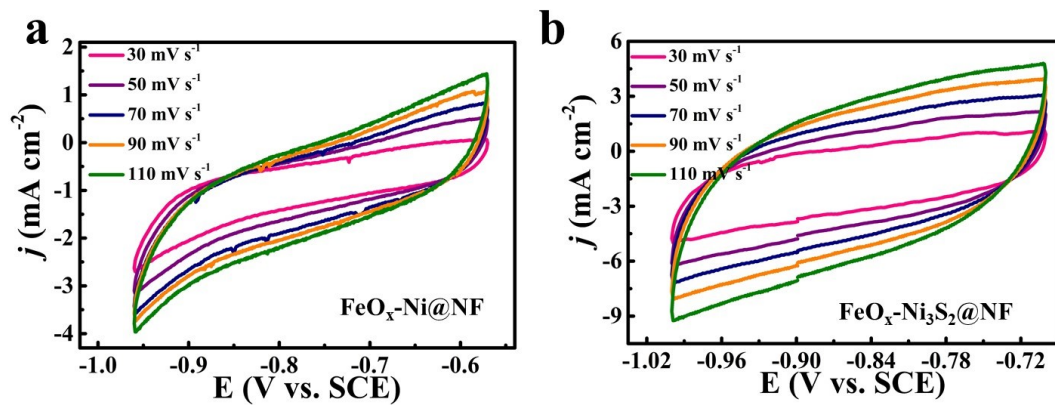


Figure S10. Cyclic voltammograms of (a) $\text{FeO}_x\text{-Ni@NF}$ and (b) $\text{FeO}_x\text{-Ni}_3\text{S}_2\text{@NF}$ electrode in the non-Faradaic current range at scan rates of 10, 30, 50, 70 and 90 mV s^{-1} for HER.

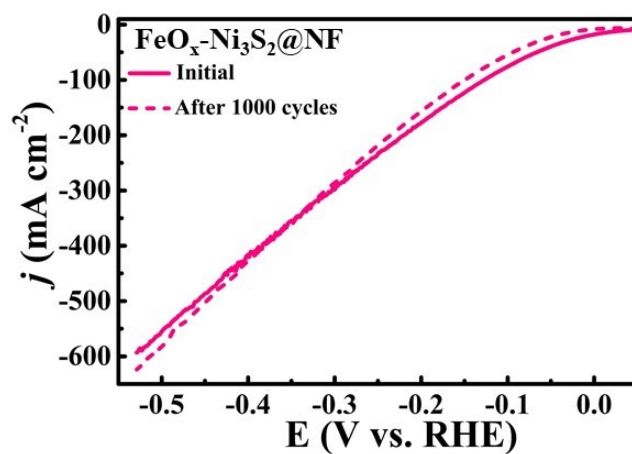


Figure S11. The LSV curves of $\text{FeO}_x\text{-Ni}_3\text{S}_2\text{@NF}$ electrode before and after 1000 CV cycles for HER.

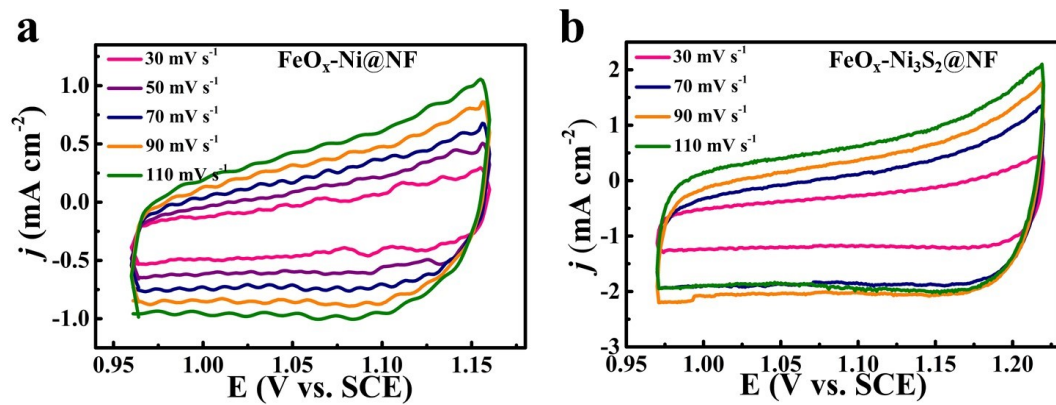
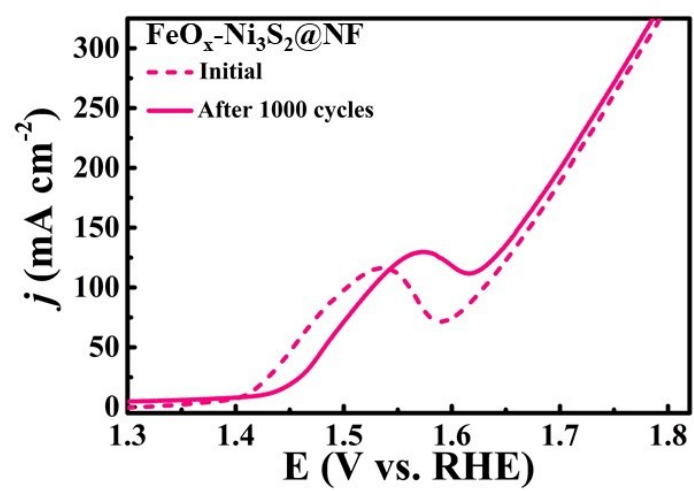


Figure S12. Cyclic voltammograms of (a) $\text{FeO}_x\text{-Ni@NF}$ and (b) $\text{FeO}_x\text{-Ni}_3\text{S}_2\text{@NF}$ electrode in the non-Faradaic current range at scan rates of 30, 50, 70, 90 and 110 mV s $^{-1}$ for OER.



FigureS13. The LSV curves of $\text{FeO}_x\text{-Ni}_3\text{S}_2\text{@NF}$ electrode before and after 1000 CV cycles for OER.

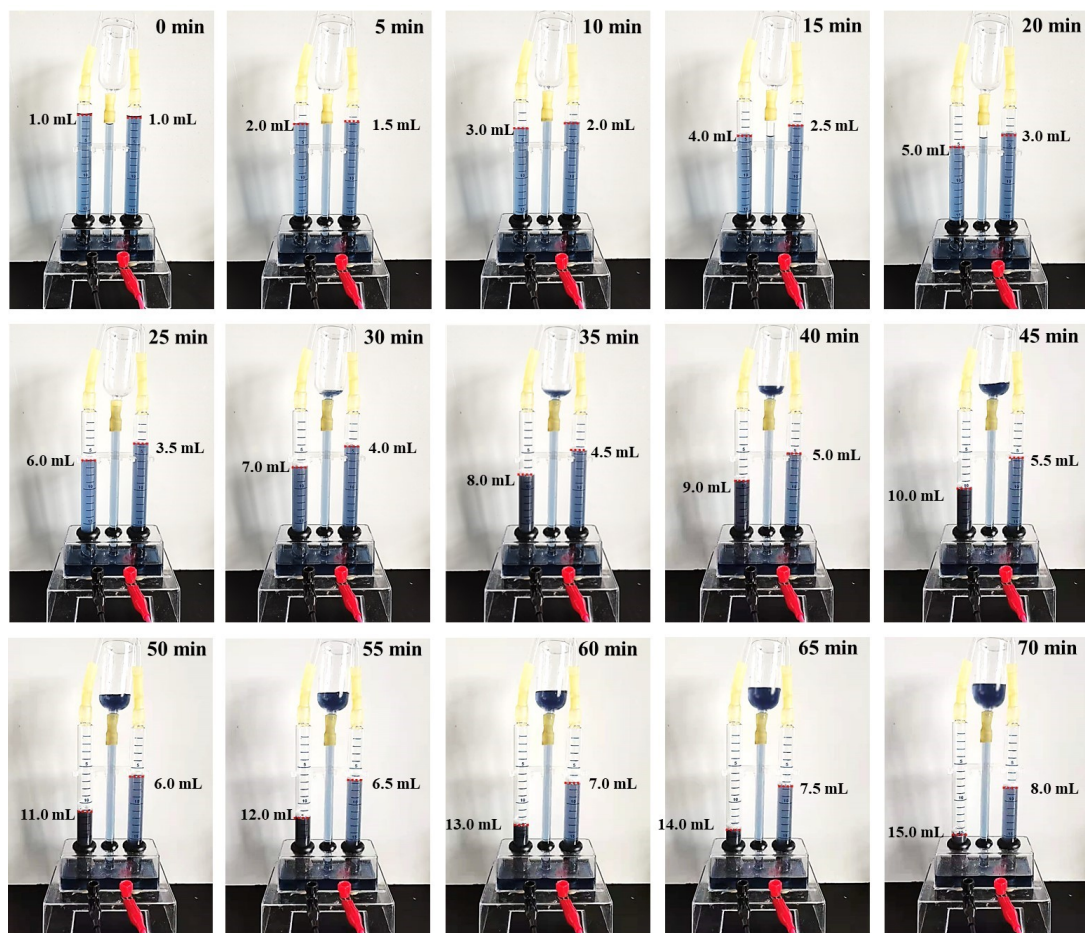


Figure S14. Collection of hydrogen (H_2) and oxygen (O_2) in water splitting in 1.0 M KOH+0.5 M NaCl at the 100 mA cm^{-2} .

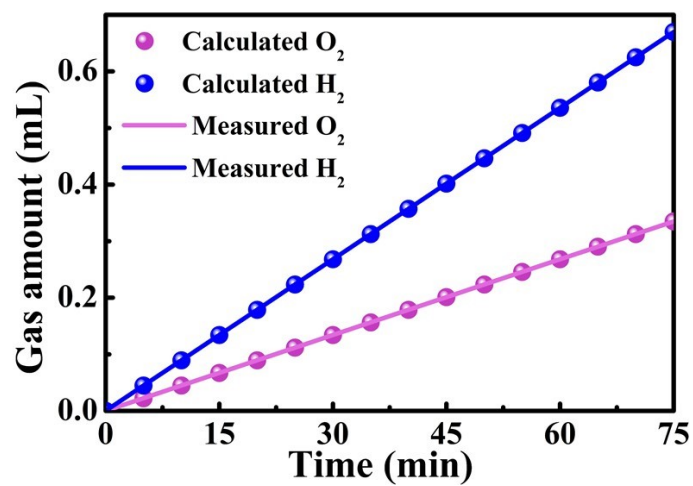


Figure S15. Amount of gas theoretically calculated and experimentally measured versus time for FeO_x-Ni₃S₂@NF || FeO_x-Ni₃S₂@NF.

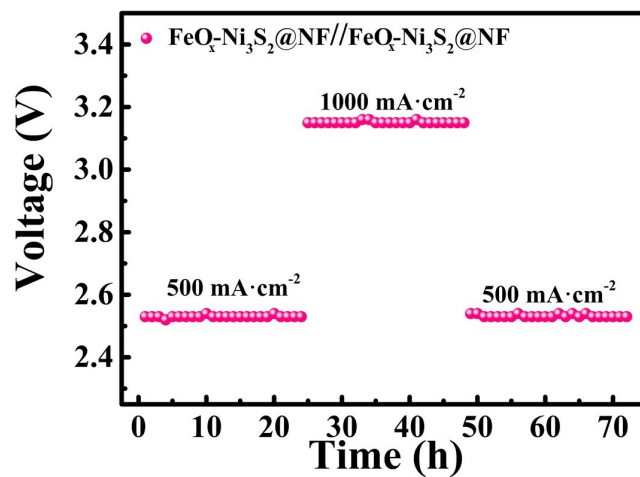


Figure S16. Long-term stability test of $\text{FeO}_x\text{-Ni}_3\text{S}_2\text{@NF}$ electrode at current densities of 500 mA cm^{-2} , 1000 mA cm^{-2} and 500 mA cm^{-2} for overall water splitting in 1.0 M KOH+0.5 M NaCl over 72 h.

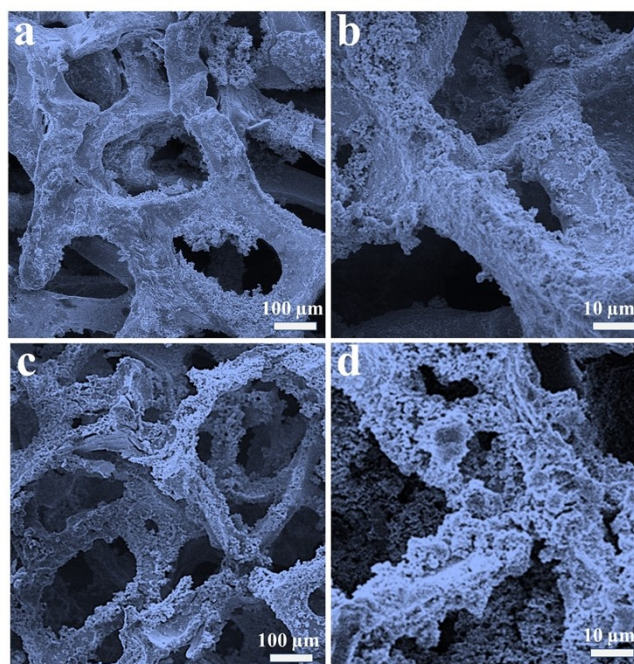


Figure S17. The SEM of $\text{FeO}_x\text{-Ni}_3\text{S}_2\text{@NF}$ electrode for HER (a, b) and OER (c, d) at 200 mA cm^{-2} in $1.0 \text{ M KOH}+0.5 \text{ M NaCl}$ after 100 h.

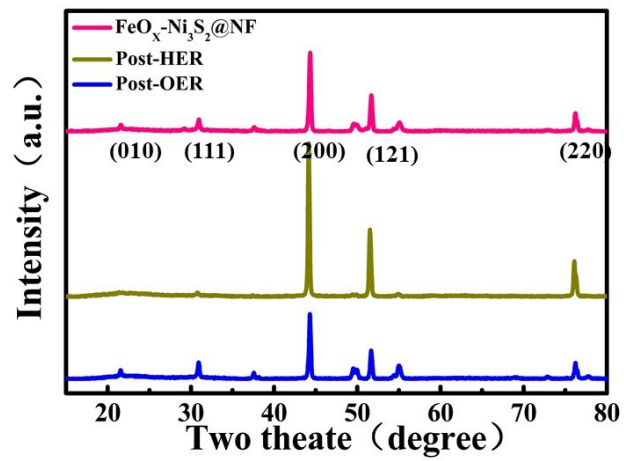


Figure S18. The XRD of $\text{FeO}_x\text{-Ni}_3\text{S}_2\text{@NF}$ electrode for HER and OER at 200 mA cm^{-2} in 1.0 M KOH+0.5 M NaCl after 100 h.

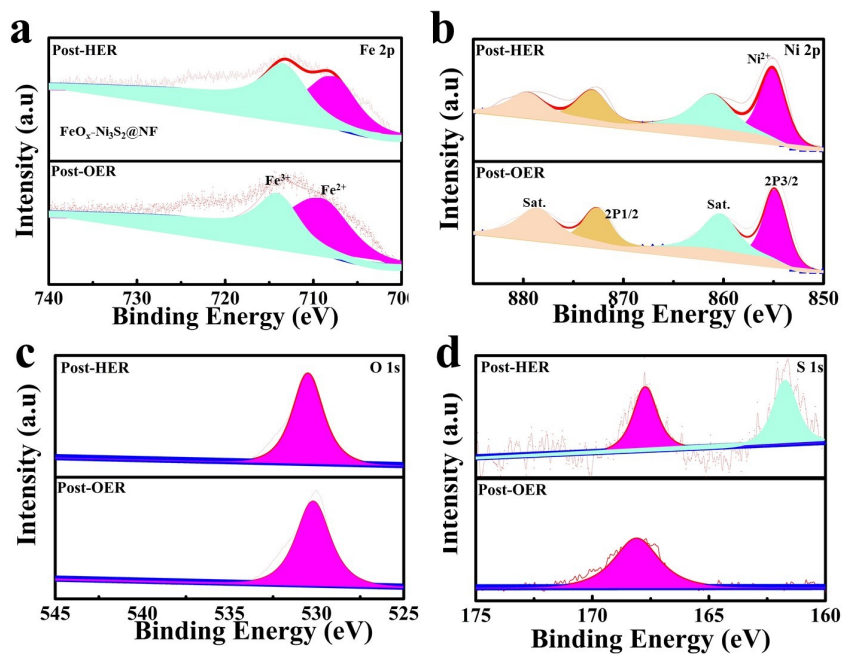


Figure S19. High-resolution XPS of $\text{FeO}_x\text{-Ni}_3\text{S}_2\text{@NF}$ electrodes for HER and OER at 200 mA cm^{-2} in $1.0 \text{ M KOH}+0.5 \text{ M NaCl}$ after 100 h. (a) Fe2p; (b) Ni2p; (c) O1s and (d) S1s.

Catalyst	State	Atomic Ratio Fe : S
FeO_x-Ni₃S₂@NF		1:4.9
	Post-HER	1:4.1
	Post-OER	1:3.4

Table S1. ICP-AES analysis of the FeO_x-Ni₃S₂@NF electrode

Table S2. Comparison the HER performance of FeO_x-Ni₃S₂@NF electrode with other electrocatalysts in 1.0 M KOH.

Catalysts	j (mA cm ⁻²)		Taf slope (mV dec ⁻¹)	References
	10	100		
FeO_x-Ni₃S₂@NF	52	178	57	This Work
Ni Foam/P-CoMoO ₄ -350	94	197	93	Adv. Sci. 2020 , 7, 1903674
H-MoS ₂ /MoP	92	-	59.8	Small 2020 , 16, 2002482
NiO/Ru@PNS	39	-	75	J. Mater. chem. A, 2019 , 7, 2344-2350
H-NiFe LDH	59	-	62.3	Energy Environ. Sci., 2019 , 12, 572-581
Pt/np-Co _{0.85} Se	55	-	35	Nature Communications, 2019 , 10, 1743
MoS ₂ -MoP/NC	35	69	30	Nano Energy, 2020 , 78, 105253
Co, Mo ₂ C-CNF	128	-	60	Chemical Engineering Journal 2020 , 125481
MoP/0.5CM-CDs1100	70	-	77.49	Nano Energy 2020 , 72, 104730
CC@N-CoP	42	-	41.2	Adv. Mater. 2018 , 1800140
Mo ₂ N /CeO ₂ @NF	26	-	37.8	ACS Appl. Mater. Interfaces 2020 , 12, 26, 29153-29161
b-S-Ni ₃ Se ₄ Se-Ni ₃ S ₂ /NF	89	-	61	Nano Energy 2020 , 74, 104787
Ni ₂ P-Ni ₁₂ P ₅ / NF	76	147	68	Small 2020 , 06770
VS ₂ -Mo-10	243	-	52.6	Chemical Engineering Journal 2020 , 396 125227
Re _{1-x} Mo _x Se ₂	77	-	42	ACS Nano 2020 , 14, 9, 11995–12005
Mo ₆ Te ₆ /MoS ₂ (1-x) Te _{2x}	320	-	55.7	Small 2020 , 2004296
N-LDH/2D-Pt	31	-	32.3	ACS Nano 2020 , 14, 8, 10578–10588
Ru SAs-Ni ₂ P	57	-	75	Nano Energy 2020 , 105467
Fe-Ni ₃ S ₂ @FeNi ₃	105	-	69	Chemical Engineering Journal 2020 , 396, 125315
(Ni _{0.75} Fe _{0.25}) ₂ P@GCs	83	-	70.4	J. Mater. Chem. A, 2019 , 7, 20357-20368
CoNi/CoFe ₂ O ₄ /NF	82	189	45	J. Mater. Chem. A, 2018 , 6, 19221-19230
NiO/Ru@PNS	39	-	75	J. Mater. Chem. A, 2019 , 7, 2344-2350

Table S3. Comparison the OER performance of FeO_x-Ni₃S₂@NF electrode with other electrocatalysts in 1.0 M KOH.

Catalysts	OER (10 mA cm ⁻²)	Tafel Slope (mV dec ⁻¹)	References
FeO _x -Ni ₃ S ₂ @NF	196	62	This work
CoNi-OH	270	73.5	Chem. Eng. J. 2020 , 401,126092
Ru-HPC	310	60.7	Nano Energy 2019 , 58, 1-10
FeNi ₃ S ₂ /NF	214	42	ACS Catal. 2018 , 8, 5431-5441
NiFeMo	238	35	ACS Energy Lett. 2018 , 3, 546-554
NiCoP@NC NA/NF	215	70.5	Adv. Funct. Mater. 2019 , 29, 1906316
δ-FeOOH NSs/NF	265	36	Adv. Mater. 2018 , 30, 1803144
Ni ₂ P-VP ₂	220	49	Adv. Mater. 2019 , 31, 1901174
Ni/Ni(OH) ₂ @NF	270	53	Adv. Mater. 2020 , 32, 1906915
Ni-Fe-Mo/NF	255	35	Adv. Sci. 2020 , 7, 1902034
Ni-ZIF/Ni- B@NF	234	76	Adv. Energy Mater. 2020 , 10, 1902714
Ni/FeOOH@NF	239	70.5	J. Mater. Chem. A, 2020 , 8, 12603–12612
YP-Co(OH)F	238	67	Small 2019 , 15, 1904105
Co ₆ W ₆ C@NC	286	53.96	Small 2020 , 16, 1907556
Ni-Ni ₃ C/CC	299	43.8	Small 2020 , 16, 2001642
Fe _x Ni _{3-x} S ₂ @NF	252	64	Adv. Energy Mater. 2020 , 10, 2001963
NiFe LDH	187	34.42	Energy Environ. Sci., 2019 , 12, 572-581
2D NiCoFe/NF	240	58	Nanoscale, 2018 , 10, 12975–12980

Table S4. The overall-water splitting performance for FeO_x-Ni₃S₂@NF and other electrodes with NF-base electrocatalysts in 1.0 M KOH.

Catalysts	Current Density (mA cm ⁻²)		References
	10	100	
FeO_x-Ni₃S₂@NF	1.41	1.61	This Work
CoNi/CoFe ₂ O ₄ /Ni	1.57	1.75	J. Mater. Chem. A, 2018 , 6,19221
MoS ₂ /Co ₉ S ₈ /Ni ₃ S ₂ /Ni	1.54		J. Am. Chem. Soc. 2019 , 141, 10417–10430
NiFeMo/NF	1.45		ACS Energy Lett. 2018 , 3, 546–554
FePO ₄ /NF	1.54	1.72	Adv. Mater. 2017 , 29, 1704574
Ni-Ni(OH) ₂ /NF	1.59		Adv. Mater. 2020 , 32, 1906915
NiFeMoOOH/NF	1.5	1.63	Adv. Sci. 2020 , 7, 1902034
Ni-ZIF/Ni-B@NF	1.54		Adv. Energy Mater. 2020 , 10, 1902714
NiP ₂ /Ni ₂ P@Ni	1.54		J. Am. Chem. Soc. 2019 , 141, 10417–10430
YP-Co(OH)F	1.54		Small 2019 , 15, 1904105
Co ₆ W ₆ C@NC	1.585		Small 2020 , 16, 1907556
Ni-Ni ₃ C/CC	1.64		Small 2020 , 16, 2001642
Ni/Ni(OH) ₂ /NF	1.59		Adv. Mater. 2020, 32, 1906915
NiFe-Mo/OOH@NF	1.5	1.63	Adv. Sci. 2020 , 7, 1902034
h-NiS _x /NF	1.54	1.72	Adv. Mater. 2017 , 29, 1704574
δ-FeOOH NSs/NF	1.62		Adv. Mater. 2018 , 30, 1803144
NixCo _{2-x} P@NC	1.56		Adv. Funct. Mater. 2019 , 29, 1906316
Fe-Ni ₃ S ₂ /NF	1.54		ACS Catal. 2018 , 8, 5431–5441
Ni ₃ N-VN/NF	1.51		Adv. Mater. 2019 , 31, 1901174
Ni/Mo ₂ C(1:2)-NCNFs	1.64		Adv. Energy Mater. 2019 , 9, 1803185